

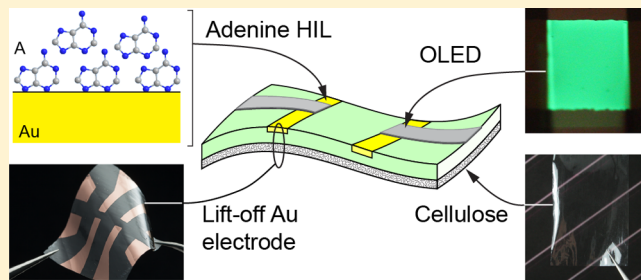
# Improved Performance of OLEDs on Cellulose/Epoxy Substrate Using Adenine as a Hole Injection Layer

Eliot F. Gomez and Andrew J. Steckl\*

Nanoelectronics Laboratory, University of Cincinnati, Cincinnati, Ohio 45221-0030 United States

**ABSTRACT:** Organic light-emitting diodes (OLED) fabricated from all “natural” materials will lead to renewable, sustainable, and potentially inexpensive organic optoelectronics. Achieving this goal will require reimagining all the various aspects of the OLED with natural-based renewable materials. Here, we replace the common substrate, electrode, and hole injection layer in the OLED structure with cellulose, gold, and the DNA nucleobase adenine. Gold films are used as semitransparent electrodes on plant-based cellulose substrates, providing flexible anodes that are highly conductive without annealing. A lift-off fabrication method (template stripping) employed UV curable epoxy to transfer patterned gold from silicon to cellulose. The gold has excellent adhesion to the epoxy (is not damaged when wiped), and the two serve as a smoothing layer for the cellulose substrate, resulting in very uniform OLED emission. DNA and DNA nucleobases are demonstrating to be versatile materials in natural electronics due to their wide energy level range. We found that adenine as a hole injection layer on gold can overcome challenges of charge injection into the organic semiconductors, increasing OLED maximum luminance and emission efficiency 4–5× on both glass and cellulose substrates through increases in current (hole injection): on glass, from ~12500 to 45000 cd/m<sup>2</sup> and from 5 to ~32 cd/A; on cellulose, from ~2000 to 8400 cd/m<sup>2</sup> and from 3 to ~14 cd/A. These results expand the utility of the DNA bases for naturally based electronics and demonstrate practical methods to integrate cellulose as a biodegradable substrate.

**KEYWORDS:** OLED, adenine, Au, bioelectronics, cellulose, flexible



Natural electronics (bioelectronics) envision a future of organic electronic devices (OLEDs, OFETs, OPVs) composed entirely (or primarily) of naturally occurring materials.<sup>1,2</sup> Organic electronics that are “all natural” would originate from renewable and inexpensive biological sources and would allow for low-cost, high-volume, expendable electronic devices. Additionally, natural electronics would be biodegradable, nontoxic, and encourage environmental stewardship and sustainability. An OLED comprised entirely of natural materials is unlikely in the near term, but considering that the harvest is plentiful for materials with intrinsically fine-tuned properties,<sup>3</sup> it may not be a matter of creating the perfect organic semiconductors and other components as much as finding them. Even though natural electronics is a nascent field, an all-natural OFET (except for the metal electrodes) made from common household ingredients has already been demonstrated,<sup>4</sup> a powerful motivation to pursue other natural electronic devices, such as the OLED.

OLEDs require multiple layers with precise electronic properties that block, inject, transport, and recombine holes/electrons to emit light. A formidable task lies ahead to find naturally based materials that serve in each of those roles. DNA has been the main biomaterial available to OLEDs,<sup>5</sup> while a few other materials, such as silk<sup>6,7</sup> as a transparent substrate, have occasionally been explored. DNA has been primarily utilized as an electron-blocking layer to increase device efficiency and luminance.<sup>8,9</sup> Our previous work<sup>10,11</sup> in natural-based OLEDs

has shown that the nucleic acid bases (nucleobases) contained in the DNA biopolymer are a versatile set of materials for the OLED for several reasons: wide range of energy levels,<sup>12</sup> readily thermally evaporated, require no additional modification. The diversity in properties of the nucleobases not only enhance the OLED performance, as in previous DNA-based OLEDs, but replace two primary OLED layers, the electron blocking layer (EBL) and the hole blocking layer (HBL), to pave the way toward an OLED derived entirely from natural or nature-inspired materials. To continue the work in all-natural OLEDs, we have focused on replacing the archetypical substrate/electrode (glass/ITO) with natural materials: plant-based paper was used as the substrate, gold was used a semitransparent electrode, and the DNA base adenine (C<sub>5</sub>H<sub>5</sub>N<sub>5</sub>) was used as a novel hole injection layer.

Paper is made of cellulose extracted from wood pulp or plant-based fibers. Cellulose is one of the most abundant raw biomaterials on the planet, making it a compelling renewable and biodegradable resource.<sup>13</sup> In addition to being lightweight and flexible, paper is significantly lower in cost compared to glass and most plastics. Paper can take on a variety of properties depending on how it is processed. For example, unlike conventional paper stock, reconstituted cellulose has high

Received: December 22, 2014

Published: February 18, 2015

optical transparency, making it an attractive alternative substrate for bottom-emitting OLEDs.<sup>14–17</sup> Because of its mechanical properties and history with mass production printing, paper is being increasingly studied for its potential applications in electronics, both as a substrate and as device components.<sup>18,19</sup>

Gold was employed here as the semitransparent electrode to replace ITO as a natural and nontoxic element. The flexible Au electrode pairs well with cellulose substrates by using a simple lift-off fabrication method with epoxy. ITO has been the dominant transparent anode for OLEDs due to its good conductivity, optical transparency, and hole injection into conventional organics. However, ITO does have its shortcomings: it requires high annealing temperatures (>300 °C) to obtain suitable conductivity and it is a brittle electrode restricting substrate flexibility.<sup>20</sup> It is likely that ITO will not be compatible for future organic devices on paper or plastic substrates.

On the other hand, Au has excellent conductivity (nearly 2 orders of magnitude higher than ITO),<sup>21</sup> which is crucial for large area OLEDs.<sup>22</sup> Au electrodes require  $\sim 5\times$  less material (thickness) to achieve the same sheet resistance as ITO, which results in a similar cost. Au does not need to be annealed and is adaptable to a variety of deposition methods, including roll-to-roll processing.<sup>23</sup> Thin film Au is semitransparent and creates a strong optical microcavity, which can deviate from Lambertian emission. However, this has been overcome through thickness optimization and high refractive index materials.<sup>24</sup> Another challenge is the strong interfacial dipole that Au forms with conventional organic molecules that result in poor metal–organic hole injection.<sup>25</sup> Interface layers of materials, such as CuPc, C<sub>60</sub>, and m-MTDATA, have been reported to improve the poor interface.<sup>21</sup> In this work we show that the DNA nucleobase adenine deposited on gold is a good hole injector into the organic layers of the OLED structure. Adenine on Au increased the hole current and also enhanced the overall OLED efficiency and luminance compared to reference devices without the nucleobase.

## FABRICATION PROCEDURE

A template stripping method for transferring Au electrodes on to cellulose was employed. The fabrication procedure of the gold anode was adapted from previously reported methods.<sup>26,27</sup> Template stripping has been used with silver electrodes for top-emitting OLEDs.<sup>28</sup> However, this is the first example of template stripping for bottom-emitting OLEDs using thin gold as the electrode to passivate cellulose or plastic substrates. Template stripping guarantees that the gold conforms its surface to the silicon surface and not to the rough cellulose substrate. It has been shown that template stripping is superior to direct evaporation for achieving very smooth gold surfaces.<sup>18,19,27</sup> In this work, gold anodes were patterned on a silicon wafer and were lifted-off onto a cellulose substrate using a UV curable epoxy (Loctite 352). The UV curing requires no heating of the paper substrate, whose decomposition begins above 150 °C.<sup>15</sup> The epoxy material used is not a natural-based polymer, but is considered nontoxic after polymerization.<sup>29</sup> Natural-based epoxy with silk<sup>30</sup> may be an interesting alternative for future work.

Figure 1 illustrates the lift-off procedure of the Au film onto the cellulose substrate. The process started with a Si wafer cleaned by oxygen plasma (Plasma-Preen, Terra Universal Inc., 500 W) for 10 min. The Au (Kurt J Lesker, 99.999%) layer was

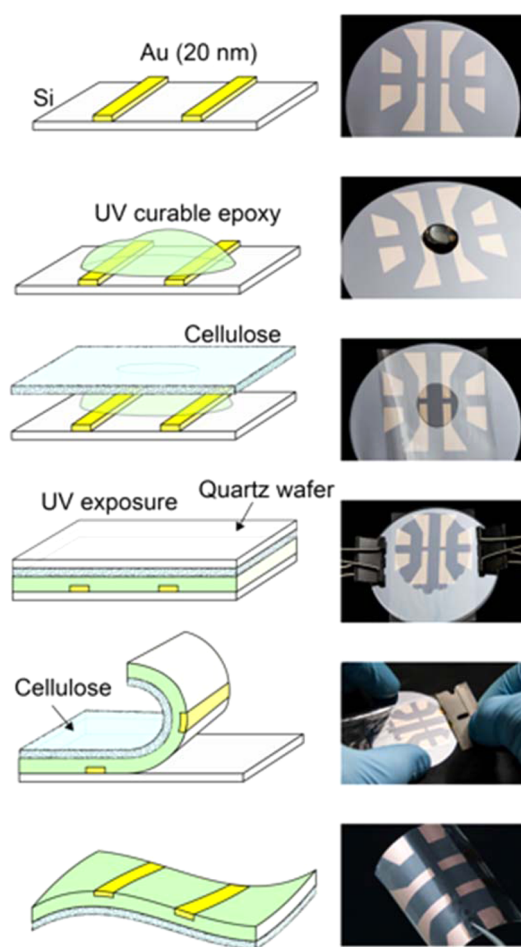


**Figure 1.** Diagram and photographs of the process of template stripping Au evaporated on silicon and transferred onto cellulose using UV curable epoxy. Template stripping ensures that the Au surface takes on the smooth Si morphology and not the rougher cellulose texture.

deposited by thermal evaporation (Edwards Coating System E306A) onto a Si wafer through an anode shadow mask. Au was deposited to a thickness of 20 nm, monitored by a quartz crystal. The Au electrode thickness was chosen based on previous work that optimized Au for transparency and sheet resistance.<sup>21,24</sup>

The transparent cellulose substrates (BBK, LLC) were  $\sim 25$   $\mu\text{m}$  thick. The Si wafer with the patterned Au was removed from the system and epoxy was dispensed directly on top of the Au. A cellulose substrate was placed on top of the epoxy and a quartz wafer was used to compress and spread the epoxy uniformly over the entire surface. The substrate was placed in a vacuum chamber to remove air bubbles from the epoxy prior to exposure, which led to improved results and lower base pressures during OLED fabrication. The cellulose is semitransparent to ultraviolet light and the epoxy cured in 2 min under a UV lamp without heat. The thickness of the epoxy was measured to be  $\sim 100$   $\mu\text{m}$ . The quartz wafer was removed after UV exposure. A razor blade was used to initiate the separation of the cellulose/epoxy/Au stack from the Si substrate. Afterward, the stack peeled off without difficulty. There was no remaining Au on the Si wafer (where the epoxy was present) and any residue could be cleaned and the wafer reused. The Au

sheet resistance on the cellulose/epoxy/Au structure was measured with a four-point probe to be  $5.5 \Omega/\square$ .

The notable benefit of the template stripping method was the improved Au adhesion to the epoxy, as demonstrated in Figure 2. Au directly evaporated on glass (or plastics) has notoriously

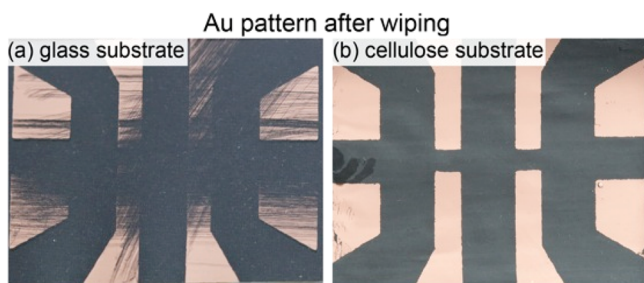


**Figure 2.** Comparison of the robustness of Au directly evaporated on glass and Au that was stripped from Si and transferred to cellulose. Gently wiping with a tissue showed that the Au layer on glass was easily removed, while the Au on epoxy/cellulose sustained no damage.

poor adhesion, often requiring additional thin metal adhesion promoters (such as Ni or Cr), which reduces the optical transmission. Figure 2a shows Au evaporated on a glass wafer that was easily damaged by wiping with a tissue. The same wiping procedure on the cellulose/epoxy/Au shows no evidence of damage in Figure 2b. Furthermore, the gold sheet resistance was maintained at  $5.5 \Omega/\square$ .

Figure 3 shows a comparison of the rough cellulose paper to the smooth gold electrodes after template stripping. Analysis of the surface quality was performed using electron microscopy (EVEX) and contour optical microscopy (Bruker ContourGT-K1). The SEM photographs in Figure 3a revealed that the surface morphology of the as-received cellulose contains large trenches ( $>25 \mu\text{m}$  wide) and other features. This was supported by the contour microscopy photographs, which shows the nonuniformity of the cellulose surface in Figure 3b. OLEDs that were fabricated on Au directly evaporated on the rough cellulose film contained a high concentration of defects, which decreased the OLED performance (Figure 3c). In the parallel experiment, Au was transferred to the cellulose by the template stripping method described above. The epoxy acts as a very efficient smoothing layer that filled the inherent defects of the cellulose. Corresponding analysis was done on the template stripped electrodes (shown in the inset of Figure 3d). The SEM and contour plots in Figure 3d and e, respectively, show that the gold layer is featureless and also confirmed by the uniform emission of the OLED fabricated on the cellulose/epoxy/Au substrate (Figure 3f). Template stripping demonstrates that specially treated cellulose or associated processes are not required for high quality OLEDs on cellulose.

The transmission spectrum was measured for each layer of the substrate/electrode (Perkin Elmer Lambda 900), as shown in Figure 4a. The results in Figure 4b show the transmission of the multiple layered cellulose/epoxy and cellulose/epoxy/Au at the same thickness used in fabrication. Au film evaporated to 20 nm on a glass substrate showed a peak transmission of 58% at 515 nm, which closely matches the green OLED emission peak at 515 nm. The cellulose film had a uniformly high transmission ( $\sim 88\text{--}90\%$ ) in the visible range, only slightly decreasing in the near-UV range to 80%. The glass substrate (1 mm) had a transmission marginally higher of 90–91% through the visible spectrum decreasing to 20% in the near-UV at 300 nm.

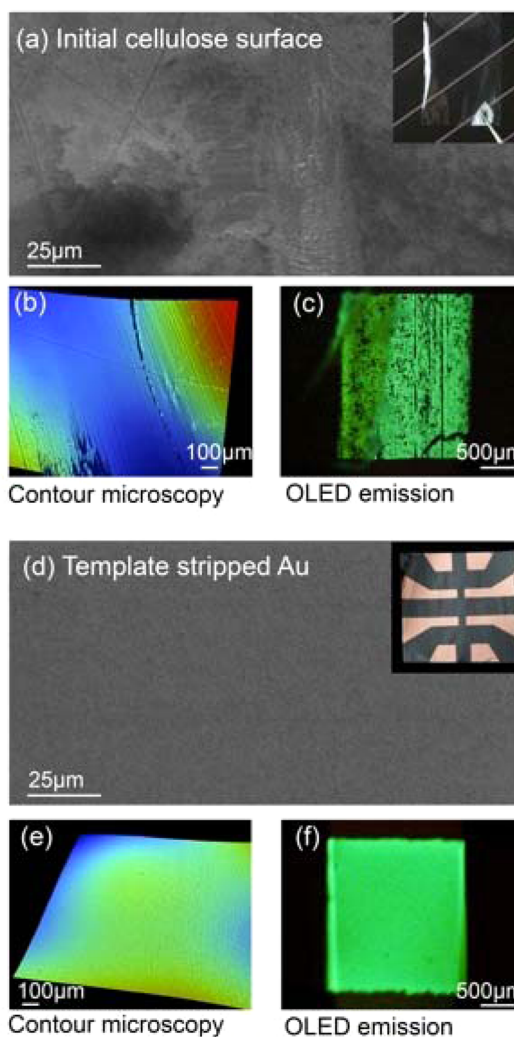


**Figure 3.** Comparison of surface morphology and OLED emission on a bare cellulose substrate and on template stripped cellulose surfaces: (a) SEM photograph of the initial cellulose surface (inset: photograph of the cellulose showing high transparency level); (b) contour microscopy image showing the rough surface of the cellulose substrate; (c) photograph of light emitting from OLED fabricated directly on cellulose showing many defects due to rough cellulose surface; (d) SEM photograph of epoxy/cellulose surface (inset: photograph of template stripped Au on cellulose) showing smooth and uniform surface; (e) contour image of the template stripped gold on cellulose; (f) defect-free OLED fabricated on template stripped gold.

Corning Willow glass ( $100 \mu\text{m}$ ) has been measured previously<sup>15</sup> to have a transmission in the visible range of  $\sim 93\%$ . The transmission plots revealed that reconstituted cellulose is optically comparable to glass and exceeds it in the near-UV range. The epoxy layer ( $100 \mu\text{m}$ ) was  $>95\%$  transparent, showing only a sharp decline below the visible spectrum ( $<400 \text{ nm}$ ). The cellulose/epoxy substrate had 87% transmission at the 515 nm, which dropped sharply in the UV due to the epoxy absorption in the UV. The addition of Au to the substrate decreased transmission to 50%, shown in Figure 4b, due to the highly reflective nature of the Au.

The lift-off procedure described above was used for the fabrication of OLEDs on cellulose substrates. The flexible substrate must lay flat during the organic deposition to minimize shadowing from the masks. Therefore, the cellulose/epoxy/Au substrate was adhered to a glass wafer

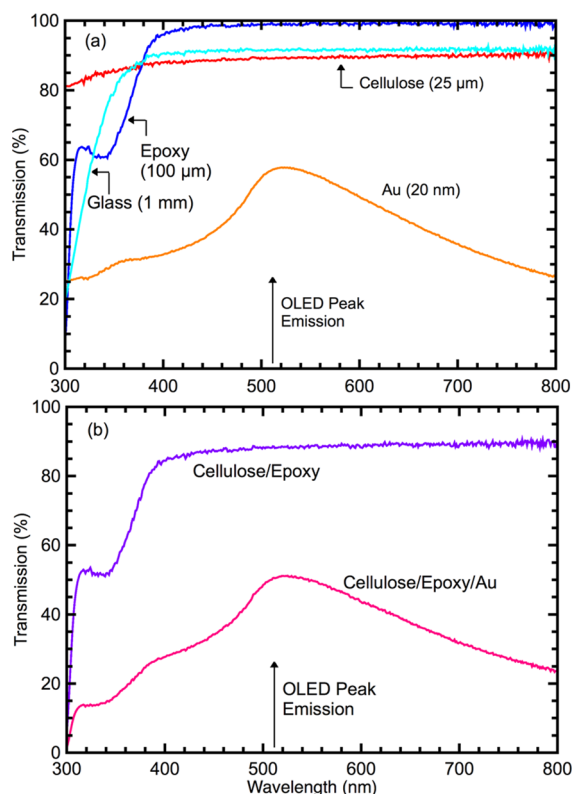


**Figure 4.** Optical transmission for materials for the thickness used in the OLED structure: (a) Au film, epoxy layer, glass substrate, and cellulose substrate; (b) cellulose with epoxy layer and cellulose/epoxy/Au.

(or PET) using epoxy during OLED fabrication. For comparison purposes, OLEDs were also fabricated wherein Au was directly evaporated on a bare glass substrate to a thickness of 20 nm.

After the substrate/electrode was prepared, the device was transferred to a multisource vacuum evaporation system (SVT Associates) for deposition of adenine (Sigma-Aldrich, 99%), organic materials (Luminescence Technology Corp. Hsin-Chu, Taiwan), and aluminum electrode. The nucleobase device (NB-OLED) was fabricated using the following layers: substrate (glass or cellulose)/Au [20 nm]/adenine [10 nm]/NPB [17 nm]/CBP:Ir(ppy)<sub>3</sub> [30 nm, 10 wt %]/BCP [12 nm]/Alq<sub>3</sub> [25 nm]/LiF [<1 nm]/Al [40 nm]. Reference devices were fabricated with the same parameters, but excluding the adenine layer. A quartz crystal microbalance monitored the organic layer thicknesses. After the device fabrication process was completed, the devices were transferred to a nitrogen-filled glovebox for characterization. Figure 5 shows the energy levels<sup>10</sup> for each of the layers and a schematic of the overall device structure on the cellulose substrate.

## RESULTS

OLED current–voltage ( $I$ – $V$ ) characterization was performed (HP-6634B DC power source) and the luminance was measured with a Konica-Minolta CS-200 luminance meter. Representative results are shown for OLEDs fabricated on glass (Figure 6a,b) and on cellulose (Figure 6c,d) substrates, with and without the adenine layer. For the OLEDs on glass substrate, the luminance and current density as a function of applied voltage are shown in Figure 6a and the current

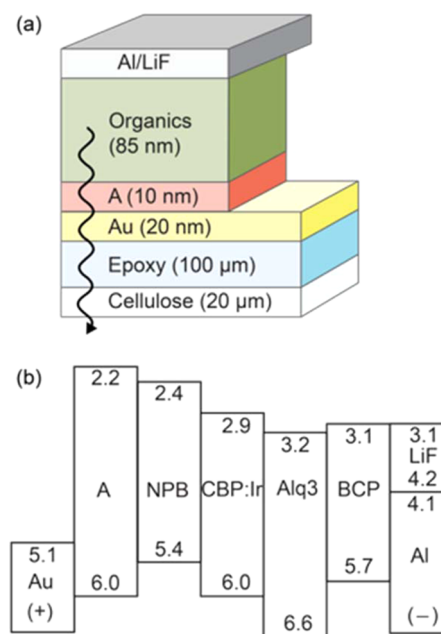


**Figure 5.** Structure of the OLED containing the Au anode and adenine (A) hole injection layer: (a) schematic of the entire stack of the OLED on cellulose showing the thickness of the stack; (b) diagram of the molecular orbital energy levels (eV) of the OLED layers.

efficiency is plotted versus luminance in Figure 6b. The OLED on glass demonstrates a significant improvement in OLED performance when a thin layer of adenine is deposited on the Au electrode. As shown in Figure 6a, the adenine OLED emitted a measurable luminance (optical turn-on) at 4.25 V, while the reference OLED turned on at slightly higher voltage of ~4.50–4.75 V. The luminance for the adenine OLED increased sharply after turn-on, reaching 100 cd/m<sup>2</sup> at 5.5 V and a maximum value of ~45000 cd/m<sup>2</sup> at 13.25 V. The reference OLED on glass obtained 100 cd/m<sup>2</sup> at 7.25 V (nearly 2 V higher than the adenine OLED) and achieved a maximum luminance of only 12500 cd/m<sup>2</sup>. The current density of the adenine OLED is uniformly higher than that of the reference device especially at lower voltages, indicating that the adenine led to improved hole injection from the Au electrode into the organic stack. This is strongly supported by a comparison of the current efficiency of the two devices. As shown in Figure 6b, the current efficiency of the adenine OLED was significantly higher than the reference device at all values of luminance, achieving a nearly 5× enhancement over the reference. This clearly indicates that adenine efficiently transported holes from the Au to the emitting layer. The adenine OLED had a peak efficiency of 31.7 cd/A and remained above 10 cd/A over most of its operating range. In comparison, the reference device without adenine has a current efficiency of less than 5 cd/A throughout the entire range.

Corresponding results for OLEDs on cellulose substrates are shown in Figure 6c,d. The results on cellulose demonstrate an even more dramatic improvement with the addition of adenine on Au. Figure 6c shows that the adenine OLED and the reference device had a turn-on voltage of 4.5 V, similar to that of the OLEDs on glass. The luminance of the adenine OLED increased sharply after turn-on reaching 100 cd/m<sup>2</sup> at 7.0 V and reached a maximum luminance of ~8400 cd/m<sup>2</sup> at 16 V. The reference OLED on cellulose obtained a luminance of 100 cd/

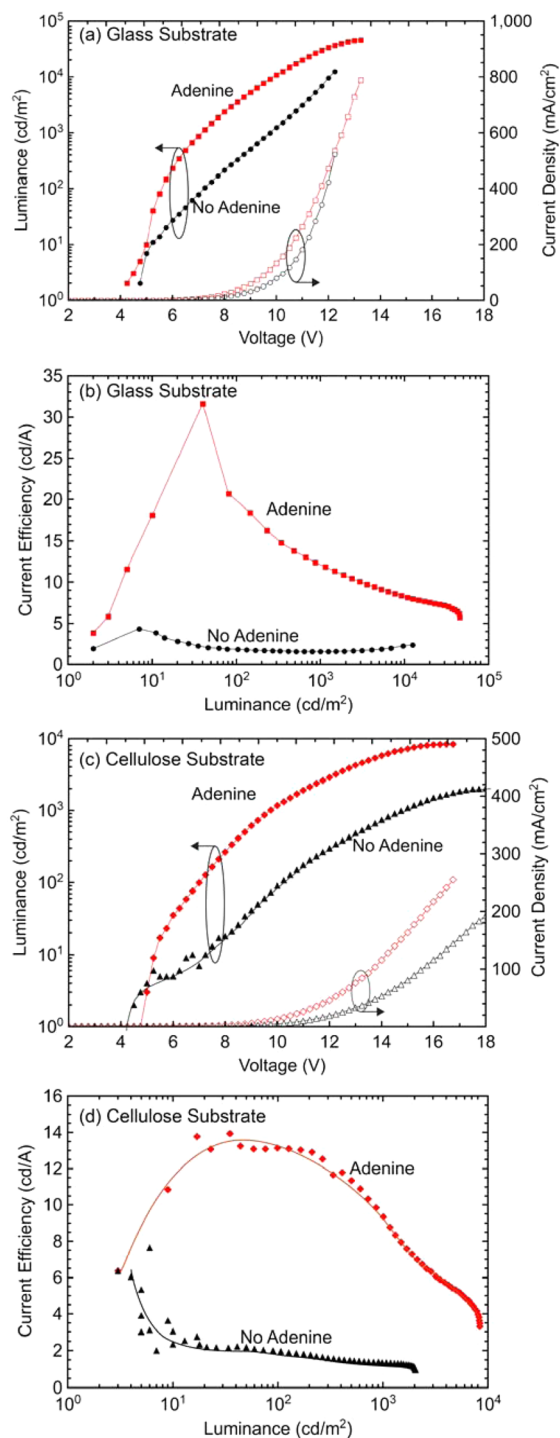


**Figure 6.** Optical performance characteristics of OLEDs with and without adenine: (a) glass substrate, luminance and current density vs voltage; (b) glass substrate, current efficiency vs luminance; (c) cellulose substrate, luminance and current density vs voltage; (d) cellulose substrate, current efficiency vs luminance.

m<sup>2</sup> at 10 V (nearly 3 V higher than the adenine OLED) and a maximum luminance of only  $\sim 2000$  cd/m<sup>2</sup>. The increase in current density for the adenine OLED over the reference device is more pronounced for the case of the cellulose substrate, as seen in Figure 6c for all values of applied voltage. The current emission efficiencies of the two OLEDs on cellulose substrate are shown in Figure 6d. The adenine OLED reached a maximum of 13.9 cd/A and remained at or above 13 cd/A up

to a luminance of  $\sim 200$  cd/m<sup>2</sup>. By comparison, the values of the reference OLED were  $< 3$  cd/A throughout most of the entire range (from  $\sim 10$  to 2000 cd/m<sup>2</sup>).

## DISCUSSION

Figure 7 plots current density versus luminance for all of the devices on glass and cellulose. It is evident that the adenine

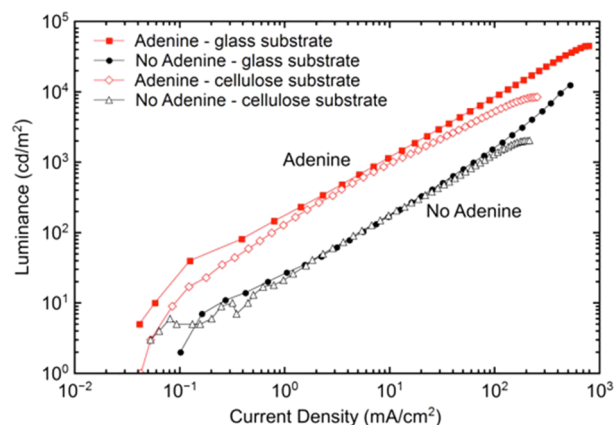


**Figure 7.** Luminance vs current density for OLEDs with and without adenine on glass and cellulose and cellulose substrates.

devices on glass and cellulose exhibit a luminance increase of nearly 8–10-fold larger over the entire current density range. We attribute the increase in performance of the adenine devices to the binding mechanisms of adenine onto the Au electrode. The binding of DNA nucleobases to gold has been extensively studied because of its importance for both fundamental studies and bionanotechnology.<sup>31–33</sup> Adenine, among the nucleobases, is reported to have an exceptionally strong physical adsorption affinity to Au.<sup>32</sup> It is interesting to compare the combination of Au and adenine as electrode/hole injection layer to that of Au and C<sub>60</sub>, which has been investigated in some detail.<sup>34,35</sup> In the Au/C<sub>60</sub> system, the barrier between the metal and organics is overcome by strong chemical reactions between the two materials<sup>34,35</sup> that cause an intimate contact, resulting in enhanced hole injection. This is similar to the strong physical adsorption of adenine on Au. It is also important to note that adenine and C<sub>60</sub> have very similar HOMO levels,  $\sim 6.0$  and  $\sim 6.2$ , respectively. Yuan et al.<sup>34</sup> has proposed that the C<sub>60</sub> layer, due to its large HOMO level, is likely to transfer holes into higher energy states in the NPB layer.<sup>34</sup> It is possible that a similar mechanism is occurring at the adenine/NPB interface.

Figure 7 also shows that the performance of devices on glass and cellulose substrates is quite similar over a wide range of bias currents. Slight loss of performance for the cellulose-based devices starts to occur at 10 mA/cm<sup>2</sup> and becoming more pronounced at 100 mA/cm<sup>2</sup> and above. The reduced maximum luminance of the cellulose-based devices suggests that local heating effects at high current may cause physical changes (such as delamination) in the cellulose/epoxy/Au interfaces. Figure 8 illustrates the operation of an adenine OLED on cellulose, while being flexed.

## CONCLUSIONS

The results presented here show several promising advancements for natural electronics in terms of fabrication methods and material selections for enhanced OLED performance on cellulose substrates. Cellulose, a natural based alternative to

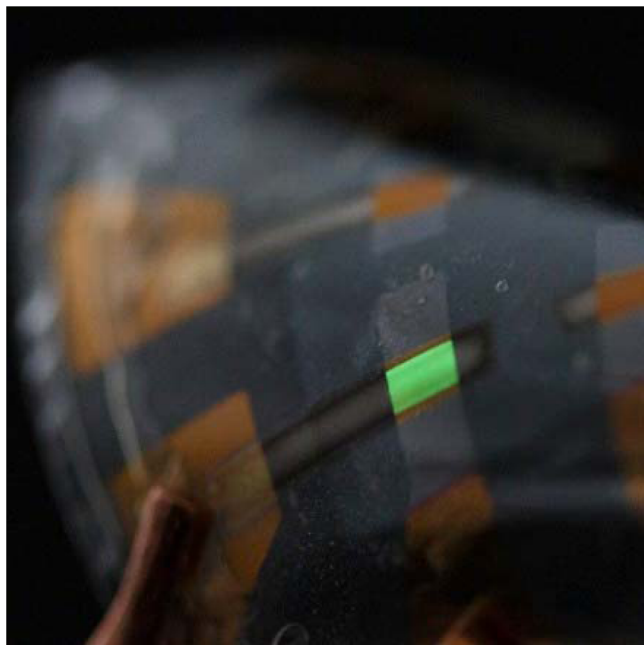


**Figure 8.** Photograph of an adenine OLED on cellulose substrate in operation while being flexed.

glass substrates for bottom-emitting OLED structures, was chosen as the substrate for its low cost, mechanical flexibility, and optical transparency. Template stripping of thin film Au using UV epoxy was a simple method that paired well with cellulose substrates to create a substrate/electrode with excellent properties: smooth electrodes, flexible, highly conductive, low temperature, excellent adhesion, and semi-transparent. In addition, it was also shown that hole injection from Au to organic semiconductors could be greatly enhanced by using the DNA nucleobase adenine. A thin layer of adenine resulted in significant improvements in current efficiency and luminance due to its intrinsic physical and chemical affinity to gold that enhanced hole injection. As natural electronics continue to advance in materials and methods, the substrate/electrode/organic combination of cellulose, gold, and adenine offer a solid foundation for future all-natural devices.

## AUTHOR INFORMATION

### Corresponding Author

\*E-mail: a.steckl@uc.edu.

### Notes

The authors declare no competing financial interest.

## ACKNOWLEDGMENTS

The authors gratefully acknowledge many useful discussions with other members of the UC NanoLab and the assistance of V. Venkatraman with some of the experiments and the support over many years from the Air Force Research Laboratory (J. Grote).

## REFERENCES

- (1) Irimia-Vladu, M. "Green" electronics: Biodegradable and biocompatible materials and devices for sustainable future. *Chem. Soc. Rev.* **2014**, *43*, 588–610.
- (2) Meredith, P.; Bettinger, C. J.; Irimia-Vladu, M.; Mostert, A. B.; Schwenn, P. E. Electronic and optoelectronic materials and devices inspired by nature. *Rep. Prog. Phys.* **2013**, *76*, 034501.

- (3) Irimia-Vladu, M.; Sariciftci, N. S.; Bauer, S. Exotic materials for bio-organic electronics. *J. Mater. Chem.* **2011**, *21*, 1350–1361.
- (4) Irimia-Vladu, M.; Troshin, P. A.; Reisinger, M.; Shmygleva, L.; Kanbur, Y.; Schwabegger, G.; Bodea, M.; Schwödau, R.; Mumyatov, A.; Fergus, J. W.; Razumov, V. F.; Sitter, H.; Sariciftci, N. S.; Bauer, S. Biocompatible and biodegradable materials for organic field-effect transistors. *Adv. Funct. Mater.* **2010**, *20*, 4069–4076.
- (5) Steckl, A. J. DNA: A new material for photonics? *Nat. Photonics* **2007**, *1*, 3.
- (6) Capelli, R.; Amsden, J. J.; Generali, G.; Toffanin, S.; Benfenati, V.; Muccini, M.; Kaplan, D. L.; Omenetto, F. G.; Zamboni, R. Integration of silk protein in organic and light-emitting transistors. *Org. Electron.* **2011**, *12*, 1146–1151.
- (7) Prosa, M.; Sagnella, A.; Posati, T.; Tessarolo, M.; Bolognesi, M.; Cavallini, S.; Toffanin, S.; Benfenati, V.; Seri, M.; Ruani, G.; Muccini, M.; Zamboni, R. Integration of a silk fibroin based film as a luminescent down-shifting layer in ITO-free organic solar cells. *RSC Adv.* **2014**, *4*, 44815–44822.
- (8) Hagen, J. A.; Li, W.; Steckl, A. J.; Grote, J. G. Enhanced emission efficiency in organic light-emitting diodes using deoxyribonucleic acid complex as an electron blocking layer. *Appl. Phys. Lett.* **2006**, *88*, 171109.
- (9) Steckl, A. J.; Spaeth, H.; You, H.; Gomez, E.; Grote, J. DNA as an optical material. *Opt. Photon. News* **2011**, *22*, 34–39.
- (10) Gomez, E. F.; Venkatraman, V.; Grote, J. G.; Steckl, A. J. DNA bases thymine and adenine in bio-organic light emitting diodes. *Sci. Rep.* **2014**, *4*, 7105.
- (11) Gomez, E. F.; Venkatraman, V.; Grote, J. G.; Steckl, A. J. Exploring the potential of nucleic acid bases in organic light emitting diodes. *Adv. Mater.* **2014**, DOI: 10.1002/adma.201403532.
- (12) Lee, J.; Park, J. H.; Lee, Y. T.; Jeon, P. J.; Lee, H. S.; Nam, S. H.; Yi, Y.; Lee, Y.; Im, S. DNA-base guanine as hydrogen getter and charge trapping layer embedded in oxide dielectrics for inorganic and organic field-effect transistors. *ACS Appl. Mater. Interfaces* **2014**, *6*, 4965–73.
- (13) Klemm, D.; Heublein, B.; Fink, H.-P.; Bohn, A. Cellulose: Fascinating biopolymer and sustainable raw material. *Angew. Chem., Int. Ed.* **2005**, *44*, 3358–3393.
- (14) Min, S.-H.; Kim, C. K.; Lee, H.-N.; Moon, D.-G. An OLED using cellulose paper as a flexible substrate. *Mol. Cryst. Liq. Cryst.* **2012**, *563*, 159–165.
- (15) Purandare, S.; Gomez, E. F.; Steckl, A. J. High brightness phosphorescent organic light emitting diodes on transparent and flexible cellulose films. *Nanotechnology* **2014**, *25*, 094012.
- (16) Ummartyotin, S.; Juntaro, J.; Sain, M.; Manuspiya, H. Development of transparent bacterial cellulose nanocomposite film as substrate for flexible organic light emitting diode (OLED) display. *Ind. Crop. Prod.* **2012**, *35*, 92–97.
- (17) Najafabadi, E.; Zhou, Y. H.; Knauer, K. A.; Fuentes-Hernandez, C.; Kippelen, B. Efficient organic light-emitting diodes fabricated on cellulose nanocrystal substrates. *Appl. Phys. Lett.* **2014**, *105*, 063305.
- (18) Tobjörk, D.; Österbacka, R. Paper electronics. *Adv. Mater.* **2011**, *23*, 1935–1961.
- (19) Steckl, A. J. Circuits on cellulose. *IEEE Spectrum* **2013**, *50*, 48–61.
- (20) Wang, G.-F.; Tao, X.-M.; Wang, R.-X. Flexible organic light-emitting diodes with a polymeric nanocomposite anode. *Nanotechnology* **2008**, *19*, 145201.
- (21) Han, S.; Yuan, Y.; Lu, Z.-H. Highly efficient organic light-emitting diodes with metal/fullerene anode. *J. Appl. Phys.* **2006**, *100*, 074504.
- (22) Helander, M. G.; Wang, Z. B.; Greiner, M. T.; Liu, Z. W.; Qiu, J.; Lu, Z. H. Oxidized gold thin films: An effective material for high-performance flexible organic optoelectronics. *Adv. Mater.* **2010**, *22*, 2037–2040.
- (23) Ohring, M. *Materials Science of Thin Films*; Academic Press: San Diego, CA, 2002.
- (24) Wang, Z. B.; Helander, M. G.; Qiu, J.; Puzzo, D. P.; Greiner, M. T.; Hudson, Z. M.; Wang, S.; Liu, Z. W.; Lu, Z. H. Unlocking the full

potential of organic light-emitting diodes on flexible plastic. *Nat. Photonics* **2011**, *5*, 753–757.

(25) Ishii, H.; Sugiyama, K.; Ito, E.; Seki, K. Energy level alignment and interfacial electronic structures at organic/metal and organic/organic interfaces. *Adv. Mater.* **1999**, *11*, 605–625.

(26) Weiss, E. A.; Kaufman, G. K.; Kriebel, J. K.; Li, Z.; Schalek, R.; Whitesides, G. M. Si/SiO<sub>2</sub>-templated formation of ultraflat metal surfaces on glass, polymer, and solder supports: Their use as substrates for self-assembled monolayers. *Langmuir* **2007**, *23*, 9686–9694.

(27) Hegner, M.; Wagner, P.; Semenza, G. Ultralarge atomically flat template-stripped Au surfaces for scanning probe microscopy. *Surf. Sci.* **1993**, *291*, 39–46.

(28) Liu, Y. F.; Feng, J.; Yin, D.; Bi, Y. G.; Song, J. F.; Chen, Q. D.; Sun, H. B. Highly flexible and efficient top-emitting organic light-emitting devices with ultrasmooth Ag anode. *Opt. Lett.* **2012**, *37*, 1796–1798.

(29) Hazard Evaluation System and Information Service. Epoxy Resin Systems. <http://www.cdph.ca.gov/programs/hesis/Documents/epoxy.pdf> (accessed Dec 18, 2014).

(30) Loh, K.; Tan, W. Natural Silkworm-Epoxy Resin Composite for High Performance Applications. In *Metal, Ceramic and Polymeric Composites for Various Uses*; Cuppoletti, J., Ed.; Intech: Winchester, U.K., 2011; pp 325–340.

(31) Demers, L. M.; Östblom, M.; Zhang, H.; Jang, N.-H.; Liedberg, B.; Mirkin, C. A. Thermal desorption behavior and binding properties of DNA bases and nucleosides on gold. *J. Am. Chem. Soc.* **2002**, *124*, 11248–11249.

(32) Kimura-Suda, H.; Petrovykh, D. Y.; Tarlov, M. J.; Whitman, L. J. Base-dependent competitive adsorption of single-stranded DNA on gold. *J. Am. Chem. Soc.* **2003**, *125*, 9014–9015.

(33) Kryachko, E. S.; Remacle, F. Complexes of DNA bases and gold clusters Au<sub>3</sub> and Au<sub>4</sub> involving nonconventional N–H···Au hydrogen bonding. *Nano Lett.* **2005**, *5*, 735–739.

(34) Yuan, Y. Y.; Han, S.; Grozea, D.; Lu, Z. H. Fullerene-organic nanocomposite: A flexible material platform for organic light-emitting diodes. *Appl. Phys. Lett.* **2006**, *88*, 093503.

(35) Veenstra, S. C.; Heeres, A.; Hadziioannou, G.; Sawatzky, G. A.; Jonkman, H. T. On interface dipole layers between C60 and Ag or Au. *Appl. Phys. A: Mater. Sci. Process.* **2002**, *75*, 661–666.